# Gamow-Teller strength distributions for nuclei in presupernova stellar cores

F. K. Sutaria* and A. Ray†
*Theoretical Astrophysics Group, Tata Institute of Fundamental Research, Bombay-400 005, India*
(Received 18 May 1995)

Electron capture and $\beta$ decay of nuclei in the core of massive stars play an important role in the stages leading to a type II supernova explosion. Nuclei in the $f$-$p$ shell are particularly important for these reactions in the post-silicon-burning stage of a presupernova star. In this paper we characterize the energy distribution of the Gamow-Teller giant resonance (GTGR) for mid-$fp$-shell nuclei in terms of a few shape parameters, using data obtained from high energy, forward scattering $(p,n)$ and $(n,p)$ reactions. The energy of the GTGR centroid $E_{\mathrm{GT}}$ is further generalized as a function of nuclear properties such as mass number, isospin, and other shell model properties of the nucleus. Since a large fraction of the GT strength lies in the GTGR region, and the GTGR is accessible for weak transitions taking place at energies relevant to the cores of presupernova and collapsing stars, our results are relevant to the study of important $e^-$ capture and $\beta$-decay rates of arbitrary, neutron-rich, $f$-$p$ shell nuclei in stellar cores. Using the observed GTGR and isobaric analog states (IAS) energy systematics we compare the coupling coefficients in the Bohr-Mottelson two particle interaction Hamiltonian for different regions of the isotope table.

PACS number(s): 97.10.Cv, 23.40.Bw, 24.30.Cz, 97.60.Bw

## I. INTRODUCTION

It is well known [1,2] that during stellar collapse the final mass of the homologously collapsing core and the strength of the subsequent type II supernova shock are determined by the final electron fraction of the core $Y_{ef}$. The latter, in turn, is influenced by the electron captures (and $\beta$ decays) taking place on the nuclei present in the core during its hydrostatic evolution, Kelvin-Helmholtz contraction, and dynamic collapse phases. This can be seen from the scaling relations [1,2] for the mass of the homologously collapsing core and for the shock energy when the core bounces at supernuclear densities:

$$M_{\mathrm{HC}} \propto Y_{ef}^2$$

and

$$E_{\mathrm{shock}} \simeq \frac{GM_{\mathrm{HC}}^2}{R_{\mathrm{HC}}}(Y_{ef}-Y_{ei}) \simeq M_{\mathrm{HC}}^{5/3}(Y_{ef}-Y_{ei}) \simeq Y_{ef}^{10/3}(Y_{ef}-Y_{ei})$$

where $M_{\mathrm{HC}}$ and $R_{\mathrm{HC}}$ are, respectively, the mass and radius of the homologously collapsing core. The electron captures and $\beta$ decays also determine the physical conditions in the (quasi)hydrostatically evolving core through their influence on the entropy per nucleon, $S_i$. This is because a low value of $S_i$ implies that (a) the number of free protons is smaller and (b) the nuclei are excited generally to low energy states. Since the core loses energy (through neutrino emission) mainly by electron captures on free protons, as a consequence of (a), the electron fraction $Y_e$ remains high leading to a more massive homologously collapsing core and subsequently a more energetic shock. Further, since the collapse is essentially adiabatic and the nuclei have low excitation energies, the low value of $S_i$ ensures that the number of drip nucleons is very small, i.e., the nucleons remain inside the nuclei right until the core reaches nuclear density. Thus, since the number of free nucleons is low, the collapse proceeds to higher densities leading to a stronger bounce shock. For all these reasons, to make a realistic model of the physical conditions prevailing in the core of a type II supernova progenitor, it is necessary to know the weak interaction rates of a number of nuclei at the relevant energies.

In general, the energy dependence of weak interaction matrix elements [or equivalently the Gamow-Teller (GT) strength distribution] is unknown for many nuclei of potential importance in presupernova stars and collapsing cores. However, for the few nuclei of interest for which the experimental data are available, it is possible to map out the energy distribution of the GT strength in terms of a few shape parameters. These parameters can be related to nuclear properties like the nuclear isospin and the mass number and a corresponding approximate distribution can be constructed for any nucleus of astrophysical interest in that nuclear shell. We consider here nuclei in the $f$-$p$ shell since in the post-silicon-burning phase the core of a presupernova massive star has a significant abundance of these neutron-rich nuclei with $A \geq 60$. In $e^-$-capture and $\beta$-decay calculations relevant to the presupernova scenario, it is not particularly important to consider the higher shells (though this is not the case during the collapse phase, where at sufficiently high density they may have nonnegligible abundances). This is because neutron shell blocking [3] (which starts at around $^{74}$Ge) substantially decreases the $e^-$-capture rate for these heavier nuclei and their contribution to the collective electron capture rates is small compared to that of mid-$f$-$p$-shell nuclei, if the latter are present with sufficient abundances.

The importance of knowing the centroid of the GT distribution ($E_{\mathrm{GT}}$) lies in the fact that it determines the effective energy of the $e^-$-capture and $\beta$-decay reactions from, e.g.,

*Electronic address: fks@tifrvax.tifr.res.in
†Electronic address: akr@tifrvax.tifr.res.in

 

the ground state of the initial nucleus to the excited state of the final nucleus, and this along with the electron Fermi energy determines which nuclei are able to capture electrons from or $\beta$-decay onto the Fermi sea at a given temperature and density — thus controlling the rate at which the abundance of a particular nuclear species would change in the presupernova core. For example, the following expression holds for the $\beta^-$-decay rates of the discrete states of the mother nucleus (see, e.g., [4]):

$$\lambda_s = \ln 2 \frac{(6250\ \text{sec})^{-1}}{G} \sum_i (2J_i+1)\exp(-E_i/kT) \times \int_0^{Q_i} \left[ |M_F^i(E')|^2 + \left(\frac{g_A}{g_V}\right)^2 |M_{\text{GT}}^i(E')|^2 \right] f(Q_i - E')dE' \quad (1)$$

where

$$G = \sum_i (2J_i+1)\exp(-E_i/kT),$$

$g_A$ and $g_V$ are the axial-vector and vector coupling constants, respectively, and the $|M_{F,\text{GT}}^i|^2$ are the corresponding Fermi and GT matrix elements. $E_i$ is the energy of the $i$th level of the mother having spin $J_i$ and $Q$ value $Q_i = Q + E_i$. The function $f(Q_i - E')$ is the phase-space factor, integrated over electron energies (in units of $m_e$) from 1 to $(Q_i - E')$. Equation (1) shows that the distributions of the transition strengths in energy are important in the rate calculations.

The $\beta$ decays can take place either through the Fermi (vector) type interaction or the Gamow-Teller (axial-vector) type interaction while the $e^-$ capture on a nucleus in the ground state involves only the GT interaction. The GT operator $G_A \Sigma_i \sigma_i t_i^{\pm}$ does not commute with the strong spin- and isospin-dependent forces of the nuclear Hamiltonian, which causes a mixing of states in both the spin as well as isospin space. While the effect of mixing in the isospin space is small (because of the relatively weaker Coulomb potential term), the mixing of states in the spin space gives rise to a broad distribution of the total GT strength in excitation energies known as the Gamow-Teller giant resonance (GTGR) which contains a large fraction of the total weak interaction strength sum. In contrast, the Fermi strength is concentrated in a narrow region of excitation energies because the Fermi operator commutes with all parts of the nuclear Hamiltonian except the Coulomb part. At temperatures and densities ($T \simeq 0.5$ MeV and $\rho \simeq 10^{10}$ g/cm$^3$) characteristic of the presupernova core, the main contribution to the weak interaction rates is expected to come from the GTGR region.

In Secs. II and III we use the available data on nuclear charge-exchange reactions on mid-$fp$-shell nuclei to characterize the GT strength distribution for arbitrary nuclei of astrophysical interest. In Sec. IV we compare our results with other theoretical methods, namely, the $M1$ method used by Klapdor [5] and the method of Fuller, Fowler, and Newman (FFN) [6]. In Sec. V we discuss the implications of the observed GT energy systematics vis-à-vis the Bohr-Mottelson two-body Hamiltonian and in Sec. VI we give our conclusions.

## II. THE GAMOW-TELLER STRENGTH DISTRIBUTION

It is well known [7,8] that the information on charge-exchange reactions in nuclei can be used to extract the GT strength distributions with respect to the excitation energy of the daughter nucleus. The charge-exchange $(p,n)$ and $(n,p)$ reactions are isospin and spin dependent over a wide range of projectile energies. The weak interaction strength distribution ($B_{\text{GT}}^+$ or $B_{\text{GT}}^-$) is propotional to the $\Delta L = 0$, forward scattering cross section in the high projectile energy, low momentum transfer limit. This can be seen by comparing the corresponding operators [9]:

$$\sum_i V_{\sigma\tau}(r_{ip})\sigma_i \cdot \sigma_p \tau_i \cdot \tau_p \quad \text{and} \quad \sum_i V_\tau(r_{ip})\tau_i \cdot \tau_p$$

which are similar to

$$G_A \sum_i \sigma_i t_i^{\pm} \quad \text{and} \quad G_V \sum_i t_i^{\pm}.$$

The $\Delta L = 0$ scattering cross sections for various mid-$fp$-shell target nuclei undergoing $(p,n)$ and $(n,p)$ reactions are reported in Refs. [10–20]. These cross sections are extracted out of the 0° spectrum by means of multipole analysis using distorted wave impulse approximation (DWIA) calculations (see Ref. [9] and references therein). The cross sections can be analyzed to obtain the experimental distribution of GT strength in energy to a reasonably good accuracy by using known calibration relations (e.g., the relation developed in [21]) and this method has been widely used in the literature [10,16].

The calculation of the weak-interaction-mediated reactions under the astrophysically relevant conditions requires the knowledge not only of the total strength in a given direction (e.g., $\beta^-$ decay or $e^-$ capture) but also of the strength distribution in nuclear excitation energy. Attempts have been made to obtain these distributions theoretically from shell model calculations. However, the number of shell model basis states can get very large for mid-$fp$-shell nuclei, even at low energies. Hence the direct method of obtaining the GTGR distribution from shell model calculation using the full $0\hbar\omega$ basis is computationally very involved even for a few nuclei. Several attempts to calculate the GT distribution from direct shell model calculations using a truncated shell model basis space have also been made (e.g., by Aufderheide *et al.* [22]) which for the above reasons, despite substantial computational efforts, are as yet approximate. We note that complete $fp$-shell $0\hbar\omega$ *Monte Carlo* calculations have been mentioned recently which show significant quenching (discussed later), and have reportedly reproduced the experimentally observed strength in nuclei such as $^{54}$Cr, $^{54}$Fe, $^{55}$Mn, and $^{56}$Fe but not in $^{58}$Ni, the result being sensitive to the interaction Hamiltonian assumed (see Koonin and Langanke [23] and references therein). In any case the calculation of the weak-interaction-mediated reaction rates for the moderately large number of nuclei required in astrophysical situations requires a straightforward and computationally manageable approach. Here, following an earlier work [4] we use the framework of a statistical approach, as in the spectral distribution theory [24,25].

The sum rule strength for a transition from an initial state $|i\rangle$ to a final state $|f\rangle$ is given by

$$S_{\sigma\tau}=\sum_f |\langle f|\sigma\tau|i\rangle|^2=\sum_f \langle i|(\sigma\tau)^\dagger|f\rangle\langle f|\sigma\tau|i\rangle$$
$$=\langle i|(\sigma\tau)^\dagger\sigma\tau|i\rangle .$$

On the single particle level, if $\langle n^P_{nlj'}\rangle$ and $\langle n^N_{nlj}\rangle$ are the fractional occupancies of the neutrons in the $nlj$ level and the protons in the $nlj'$ level, then the GT sum rule (e.g., for $\beta^-$ decay) is given by the expression

$$S^{\rm GT}_{\beta^-}=3Z_n\sum_{nljj'}|C^{jj'}_{nl}|^2(1-\langle n^P_{nlj'}\rangle)\langle n^N_{nlj}\rangle \qquad (2)$$

where $C^{jj'}_{nl}=[2(2j+1)(2j'+1)]^{1/2}W(l\,\frac{1}{2}\,j1;\ j'\,\frac{1}{2})$ and $W$ is the Racah coefficient. The occupation numbers $\langle n^P_{nlj'}\rangle$, $\langle n^N_{nlj}\rangle$, etc. in a given shell can be calculated with the spectral distribution theory (see, e.g., Refs. [24] and [25]).

For the distribution of the strength with the nuclear excitation energy we note that according to the spectral distribution theory, for a many particle space of large dimensionality, the smoothed-out eigenvalue distribution of a (2+1)-body Hamiltonian is approximately a Gaussian. A skewed Gaussian (called the Edgeworth expansion) of the form

$$B^{\pm}_{\rm GT}(x)=A_0[1+\gamma_1(x^3-3x)/6+\gamma_1^2(x^6-15x^4+45x^2-15)/72]\exp(-x^2/2)$$

where

$$x=(E_{\rm ex}-E_{\rm GT})/\sigma$$

is used here. The parameters $\gamma_1$ (the skewness factor), $E_{\rm GT}$ (the energy centroid), $\sigma$ (the effective half-width), and $A_0$ (normalization factor) are obtained for each daughter nucleus by fitting the above formula to the experimentally obtained strength distribution.

It is known that if the total strength in the $GT^+$ direction is small the observed value of the total Gamow-Teller strength in the $GT^-$ direction is, on the average, approximately 50% of the theoretically predicted value of $3(N-Z)$ (for the nuclei studied here, it is observed to vary between 45% and 63%). This quenching of GT strength given by the factor $Z_n$ in Eq. (2) above is expected to be due to the excitation of $\Delta$ isobars at higher excitation energies through $N^{-1}-\Delta$ transitions, or the missing GT strength may lie at higher excitations (between 30 MeV and 50 MeV) [8]. On the other hand, in the electron capture direction, the total GT strength sum (i.e., $\int_0^\infty B^+_{\rm GT}(E')dE'$) in the $f$-$p$ shell has been argued to depend on the number of valence protons and the number of neutron holes in the $fp$ shell [23]. According to these authors the *total* $GT^+$ strength observed experimentally in the mid-$fp$-shell nuclei can be fitted by an expression like

$$B({\rm GT}_+)=0.0429Z_{\rm val}(20-N_{\rm val}).$$

As argued by them, in the electron capture direction for nuclei having $N>Z$, the number of possible transitions is limited by the number of available neutron holes and the number of protons in the full $f$-$p$ shell. They also suggest that the neutron-proton correlations throughout all of the $f$-$p$ shell are important in reproducing the observed quenching, and mid-$fp$-shell nuclei in this sense behave as though there is only one large shell in which all subshell structure has been diluted. The above expression includes the observed quenching and can therefore be used to independently fix $Z_n$ for the sum rule for electron capture in an equation similar to Eq. (2)

TABLE I. Edgeworth parameters for $B^-_{\rm GT}$ energy distribution obtained from $p$-$n$ reactions.

| Nucleus | $A_0(B^-_{\rm GT}$/MeV) | $E^-_{\rm GT}$ (MeV) | $\sigma$ (MeV) | $\gamma_1$ |
|---|---|---|---|---|
| $^{51}$V | 1.2 | 10.7 | 4.2 | −1.00 |
| $^{81}$Br | 2.0 | 10.2 | 3.6 | −1.19 |
| $^{71}$Ga | 2.0 | 9.6 | 3.0 | −1.25 |
| $^{58}$Ni | 1.0 | 9.4 | 1.8 | 0.11 |
| $^{60}$Ni | 0.8 | 9.0 | 2.6 | 1.05 |
| $^{54}$Fe | 1.2 | 8.9 | 1.8 | −0.50 |
| $^{56}$Fe | 1.0 | 9.0 | 3.5 | −0.67 |

For reasons discussed in Sec. I and the beginning of this section, astrophysical calculations require, apart from the total $GT^+$ strength itself (such as given above), its distribution in energy — which is characterized by higher moments of the distribution such as the energy centroid $E_{\rm GT}$, the skewness of the distribution, etc. With the objective of generating the $B_{\rm GT}(E)$ distribution of any arbitrary nucleus $(A,Z)$ of potential astrophysical importance, we now make use of the experimentally available data. The $B^+_{\rm GT}(E)$ and $B^-_{\rm GT}(E)$ distributions obtained from analysis of charge-exchange experiments are least-square fitted to the Edgeworth expression discussed above, under the constraint that the total "experimental" GT strength is reproduced by the area under the fitted expression. The Edgeworth expansion gives a good fit in the cases of $^{51}$V, $^{81}$Br, $^{71}$Ga, and $^{60}$Ni. In the case of $^{58}$Ni (target nucleus), the resonance region between 7.5 and 12 MeV is fitted well by the Edgeworth expression. Similarly for $^{54}$Fe, the fit is reasonably good between 6 and 12 MeV. For these nuclei, the strength fluctuates rapidly at low excitation energy, suggesting that at these energies single particle transitions dominate over collective resonance. Since spectral distribution theory is based on a statistical description of a large number of basis states, it is not expected that the Edgeworth expansion will reproduce the fluctuating strengths at low energies due to single particle transitions. Nevertheless, for the GT collective resonance region (which is important because of the bulk of the total strength being accessible at energies relevant to the astrophysical situation), the spectral distribution theory approach is useful.

Finally, since for $^{56}$Fe, $^{54}$Fe, $^{58}$Ni, and $^{60}$Ni, only the $\sigma(L=0)$ $(p,n)$ cross section is reported in Ref. [10], the calibration relation based on the factorized DWIA expression for the $L=0$ differential cross section as developed in [21] was used to convert the reported cross section to $B^-_{\rm GT}$/MeV. Table I gives the Edgeworth parameters for each of these fits. A typical fit of $B^-_{\rm GT}$ per 0.1 MeV interval (for $^{71}$Ga) is shown in Fig. 1. The data used in these fits came from Refs. [10]

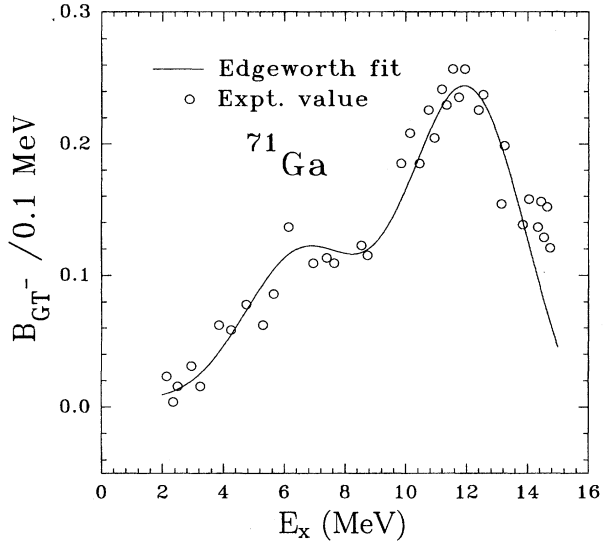


FIG. 1. The best fit Edgeworth distribution superposed on the $B_{\rm GT}^{-}$ distribution obtained from $p$-$n$ reaction on $^{71}$Ga at 120 MeV. The excitation energy $E_x$ is with repsect to the ground state of $^{71}$Ge.

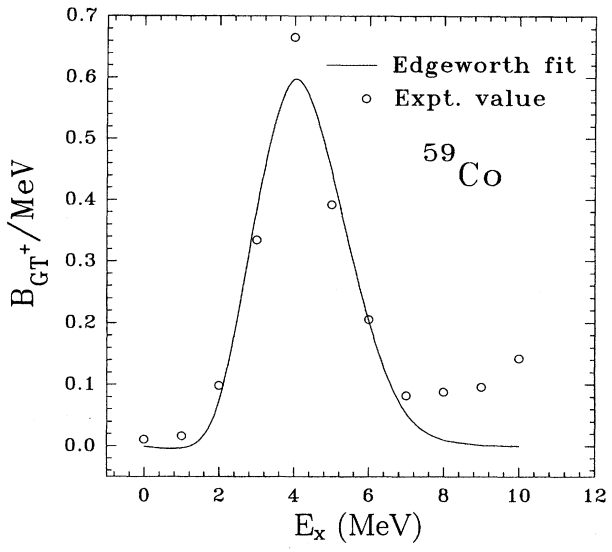


FIG. 2. The best fit Edgeworth distribution superposed on the $B_{\rm GT}^{+}$ distribution obtained from $n$-$p$ reaction on $^{59}$Co at 198 MeV.

($^{54,56}$Fe, $^{58,60}$Ni), [12] ($^{81}$Br), [13] ($^{51}$V), and [14] ($^{71}$Ga).

The Edgeworth parameters for $B_{\rm GT}^{+}(E)$ per MeV vs. $E_x$ fits are tabulated in Table II. Figure 2 shows the distribution and fit for $^{59}$Co. The distribution is well reproduced for the low energy region and the main GTGR peak. For this set of results the data were obtained from Refs. [11] ($^{54}$Fe), [16] ($^{56}$Fe, $^{58}$Ni, $^{55}$Mn), [17] ($^{51}$V, and $^{59}$Co), and [18] ($^{70}$Ge). For $^{70}$Ge, Vetterli *et al.* [18] quote the value of $B_{\rm GT}^{+}$ up to 7.6 MeV only, because of the difficulty of extraction of the $\Delta L=0$ component from the $(p,n)$ cross section. The parameters for this nucleus reported in Table II are obtained on the basis of the strength up to 7.6 MeV only. In some cases the single particle transitions may dominate in either direction at low excitation energy, and so wherever they are known experimentally these should be used explicitly in the transition rate calculations.

## III. PREDICTED CENTROIDS OF GT STRENGTH DISTRIBUTIONS

We refer to the centroids of the $B_{\rm GT}^{\pm}(E)$ distributions obtained by making Edgeworth fits to those reported from the $(p,n)$ and $(n,p)$ experiments as the "experimental centroids." In order to be able to predict such an energy distribution for any relevant $f$-$p$ shell nucleus, we relate the shape parameters for $B_{\rm GT}^{\pm}$ distributions to nuclear properties like the nuclear ground-state isospin, and the mass number. Here we report the relation developed for the energy centroid $E_{\rm GT}$, which can be applied to arbitrary nuclei of astrophysical interest for rate calculations.

TABLE II. Edgeworth parameters for $B_{\rm GT}^{+}$ energy distribution obtained from $n$-$p$ reaction data.

| Nucleus | $A_0(B_{\rm GT}^{+}$/MeV) | $E_{\rm GT}^{+}$ (MeV) | $\sigma$ (MeV) | $\gamma_1$ |
|---|---|---|---|---|
| $^{54}$Fe | 0.6 | 2.8 | 2.1 | 1.01 |
| $^{51}$V | 0.3 | 3.8 | 1.3 | −1.21 |
| $^{59}$Co | 0.6 | 4.3 | 1.2 | 0.43 |
| $^{70}$Ge | 1.0 | 2.1 | 2.1 | −1.53 |
| $^{56}$Fe | 0.6 | 2.3 | 1.8 | 0.97 |
| $^{55}$Mn | 0.4 | 4.4 | 1.9 | 0.53 |
| $^{58}$Ni | 1.0 | 3.3 | 1.5 | 0.59 |

### A. GT$^{-}$ energy systematics

The GT$^{\pm}$ operator is a space vector and an isovector, and the selection rules governing this transition require that $\Delta J=0,\pm1$, $\Delta\pi=0$ (no $0^{+}\rightarrow0^{+}$), and $\Delta T=0,\pm1$. Since the Fermi operator is a pure isovector, the selection rules require that $\Delta J=0$, $\Delta\pi=0$, and $\Delta T=0$, i.e., transitions take place only between isobaric analog states (IAS's). For both Fermi and allowed GT transitions $\Delta L=0$. It has been argued (see [26], [7], and [6]) that, under the action of resonant GT or Fermi operators, the collective states have centroids located at $E_{\rm GT}^{-}$ and $E_{\rm IAS}$ with respect to the appropriate, unperturbed state such that the difference $E_{\rm GT^-}-E_{\rm IAS}$ should depend on the spin-orbit splitting term ($\sim A^{-1/3}$), and on the isospin-dependent Lane potential term [$\sim(N-Z)/A$]. The latter gives the energy difference between two levels having the same $T_z$, but differing in $T$ by one unit. The excitation energy of the isobaric analog state $E_{\rm IAS}$ (where the Fermi centroid is located) is obtained in our analysis either experimentally (where available), or from the following theoretical relation developed by Fowler and Woosley and reported in Ref. [6] for neutron-rich nuclei:

$$E_{\rm IAS}=\Delta M_A-\Delta M_C-0.7824+\frac{1.728(Z_C-1)}{R}\ \text{MeV} \tag{3}$$

with

$$R=1.12A^{1/3}+0.78.$$

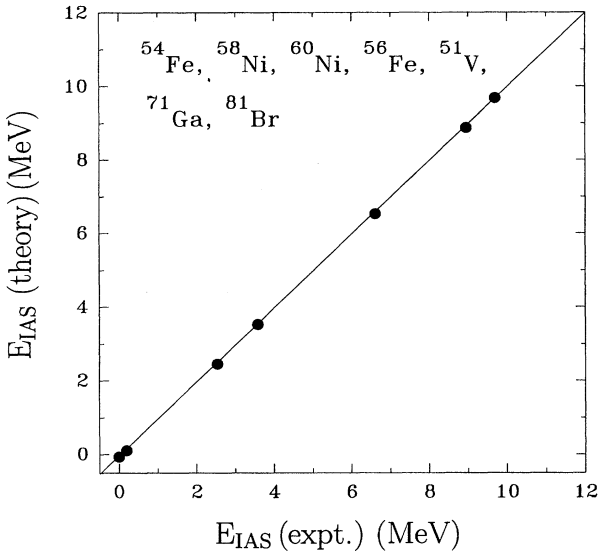


FIG. 3. Correlation between $E_{IAS}$ as calculated from Eq. (3) and the experimental positions of the IAS for $fp$ shell nuclei from $(p,n)$ reaction data. Nuclei indicated in the figure are ordered with increasing values of experimental $E_{IAS}$.

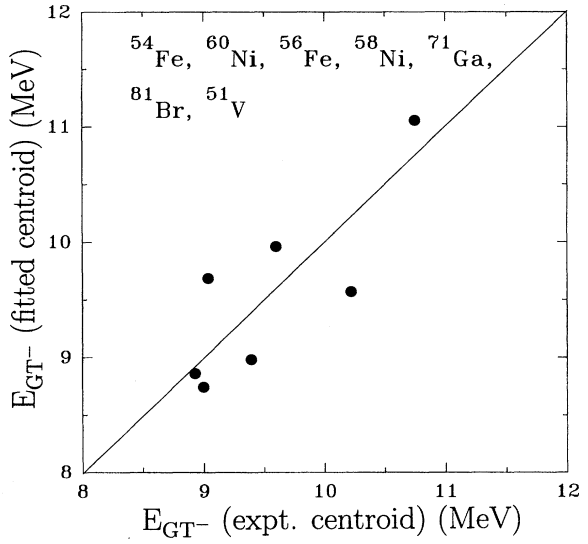


FIG. 4. $E_{GT^-}$ as obtained from Eq. (4) plotted agains the "experimental" $E_{GT^-}$ centroids. Nuclei indicated are given in order of increasing value of experimental $E_{GT^-}$.

Here $\Delta M_A$ is the mass excess of the initial nucleus, $\Delta M_C$ is the mass excess of the final nucleus, and $R$ is the radius in fm. This is observed to agree very well with the experimental data used in this work (see Fig. 3). Fitting a linear combination of the spin-orbit- and isospin-dependent terms to the experimental centroids $E_{GT}^{-}$ for the $(p,n)$ reaction data, we get the following empirical relation:

$$E_{GT^-}-E_{IAS}=44.16A^{-1/3}-76.1(N-Z)/A. \quad (4)$$

The correlation between the theoretical $E_{GT^-}$ obtained from (4) (together with the experimental values of $E_{IAS}$ reported in the references given earlier) and the experimental $GT^-$ centroids as referred to above is shown in Fig. 4. It is noted that a similar relation derived earlier [26] (also in [7]) using data for nuclei well beyond the $f$-$p$ shell had the corresponding coefficients differ substantially from those obtained in Eq. (4) for the $f$-$p$ shell nuclei. The reason for this difference is discussed in Sec. V. The goodness of the fit is measured in terms of the rms deviation from the experimental value and is evaluated to be 0.43 MeV. As is apparent from Table III and Fig. 4, the $GT^-$ centroids are located roughly between 9 and 11 MeV. This, together with the expected thermal spread of the electron Fermi distribution at temperatures relevant in the presupernova core (typically $5\times10^9$ K), and a $\sigma_N\simeq3$ MeV, would make a typical error of the order of 0.43 MeV in the predicted centroid quite acceptable for astrophysical rate calculations.

### B. $GT^+$ energy systematics

Since in the $n$-$p$ reaction there is a transition from a parent nuclear ground state having isospin $T=T_z$ to a daughter state having minimum isospin $T_d=T_z+1$ (for g.s. to g.s. transition), there can be no IAS state in the daughter corresponding to the ground state of the mother for the electron capture or the $GT^+$ direction. Thus $E_{GT^+}$ has to be obtained directly (in contrast to $E_{GT^-}-E_{IAS}$ in the $GT^-$ direction) and can be expected to depend on the spin-orbit splitting term, the Lane potential term, and for odd-$A$ nuclei, on the pairing energy term as well.

Electron capture/$e^+$ emission on a nucleus generally raise the final nucleus to an excited state. The single particle excitation configurations of most of these excited states can be constructed from its ground state by breaking either a proton or a neutron pair and raising a single particle to an excited level or by raising an unpaired single particle (if available) to an excited state. For odd-even/even-odd nuclei, the excited states of the final even-odd/odd-even nuclei (which are connected to the ground state of the parent nucleus by $GT^+$ transitions), can be generated from the g.s. of the final nucleus by breaking a particle pair in the lower energy level and using it to create an unpaired particle in a higher energy level or to pair off a previously unpaired particle in a higher energy level and simultaneously raise another single particle to the excited state. For an odd-odd/even-even initial nucleus, however, the excited states in the final even-even/

TABLE III. Experimental values of the energy centroids in MeV for $GT^-$ excitation in the mother nucleus and values obtained from the fit Eq. (4) and from the FFN method.

| Nucleus | $E_{GT^-}$ (MeV) (Expt.) | $E_{GT^-}$ (MeV) [Eq. (4)] | $E_{GT^-}$ (MeV) (FFN) |
|---|---|---|---|
| $^{51}$V | 10.7 | 11.1 | 10.6 |
| $^{81}$Br | 10.2 | 9.6 | 12.0 |
| $^{71}$Ga | 9.6 | 9.9 | 13.6 |
| $^{54}$Fe | 8.9 | 8.9 | 8.7 |
| $^{58}$Ni | 9.4 | 9.0 | 6.5 |
| $^{56}$Fe | 9.0 | 9.7 | 12.6 |
| $^{60}$Ni | 9.0 | 8.7 | 4.9 |

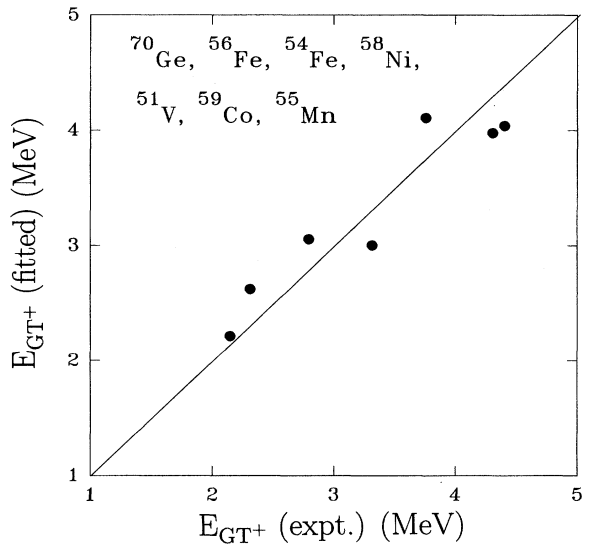


FIG. 5. $E_{GT^+}$ as obtained from Eq. (5) plotted against the "experimental" $E_{GT^+}$ centroids. Nuclei are given in order of increasing value of experimental $E_{GT^+}$.

odd-odd nucleus will be generated by breaking and making a particle pair. This implies that the energy required to break a pair in the final odd-$A$ nucleus must also be included in any expression for $GT^+$ energy systematics.

Fitting the experimental $E^+_{GT}$ centroids [obtained from the Edgeworth weighted experimental $B^+_{GT}(E)$ distributions] to a linear combination of these terms, we arrive at the following empirical relation for the $E_{GT^+}$ centroid with respect to the ground state of the final nucleus:

$$E_{GT^+} = 13.10A^{-1/3} - 11.28(N-Z)/A + 12A^{-1/2}\delta_{A_{odd}}. \quad (5)$$

The plot of $E_{GT^+}$ from (5) vs the experimental centroid is shown in Fig. 5. The goodness of fit in Fig. 5 is also measured in terms of the rms deviation from the experimental value, and has the value 0.31 MeV. The nuclei used in both figures are stated in the order of increasing $E_{GT}$ (experimental). We note that Koonin and Langanke [23] suggest that the GT resonance appears in $(n,p)$ spectra at systematically higher energies for odd-$Z$ targets than for even-$Z$ targets, although this is based on data involving target nuclei with even numbers of neutrons. On the basis of single particle excitation diagrams for the final nucleus, conforming to GT selection rules for a transition from the initial to the final nucleus, we find that the pairing energy dependence in terms of odd $A$ in Eq. (5) (the last term) will be present even in odd-$N$, even-$Z$ nuclei.

The average difference of experimental and predicted values of 0.4 MeV in $E^-_{GT}$ and 0.3 MeV in the case of $E^+_{GT}$ can be mitigated by the spread in the electron Fermi-Dirac distribution due to the 0.5 MeV temperature and also due to the fact that in a given region of the star at a particular stage of evolution there are several nuclear species present in the stellar material simultaneously. The total transition rate of this large admixture of nuclei is likely to be dominated in a given stage and region by a few nuclear species, with relatively large transition rates and abundances. These would necessarily have large energies of transition and would in any case consume a substantial fraction of the strength sum rule. Thus for astrophysical purposes the level of accuracy of the predictions for the $GT^{\pm}$ centroids obtained here is expected to be adequate.

Data for $^{45}$Sc and $^{48}$Ti are also available in Refs. [15] and [20]. However, we have not used these two nuclei in obtaining Eq. (5) and Fig. 5, partly because these nuclei are close to the beginning of the $fp$ shell where the general assumptions of the statistical nature of the spectral distribution theory may not be valid. For this reason, the calculation of the Edgeworth weighted centroid of the experimental $B_{GT^+}(E)$ distribution gives inaccurate results because of the low energy strength. Indeed, if these nuclei were to be included in Fig. 3, the goodness of fit would have decreased to a rms value of 1.37 MeV. Similarly, we had to ignore the data for $^{90}$Zr [19] because the $g_{9/2}$ shell is occupied in this nucleus. Effectively, it can be said that Eq. (5) is valid for mid-$fp$-shell nuclei with $N>Z$.

## IV. COMPARISON WITH OTHER THEORETICAL METHODS

While a detailed shell model calculation for these nuclei requires a very large number of basis states and would be difficult to carry out for each of these nuclei, it is conceivable that a reasonably good estimate of the GT excitation energy centroids can be obtained by using either the $M1$ excitation method (for the $GT^+$ excitation) or the FFN method (for the $GT^-$ excitation). These methods are described in detail in Ref. [6]. The predictions of these methods are compared with the results obtained in this paper in the following paragraphs and in Table III and Table IV.

In the FFN method, the GT transition in the $GT^+$ ($GT^-$) direction, which can be either the spin-flip (sf) or the no-spin-flip (nsf) transition, is reproduced by taking into account all possible excitations of a $p$ ($n$) in the parent nucleus to a sf or nsf orbital (for which $\Delta L=0$) and then converting the $p$ ($n$) to $n(p)$ via the $\tau^+$ ($\tau^-$) operator. The GT excitation energy for that transition is given by the sum of the excitation energies with respect to the ground state of the daughter nucleus together with the Lane potential energy and, if required, the pairing energy term. The GT centroid energy with respect to the ground state of the daughter nucleus is given by the weighted average of all these sf and nsf transitions. For example, in Fig. 6, the ground state (g.s.) of $^{51}$V is connected to the g.s. of $^{51}$Cr by a nsf $\tau^-$ transition, and to an excited state by a sf $\tau^-$ transition. For the former transition, the GT excitation energy (measured, as always, with respect to the ground state of $^{51}$Cr) equals the Lane potential $[50(N-Z)/A]$, which is evaluated as 4.90 MeV. The square of the GT matrix element for this transition is 6.42. For the latter transition, the GT excitation energy is the sum of single particle excitation energies (6.66 MeV), the Lane potential (4.90 MeV), and pairing energy (1.68 MeV), while the square of the transition matrix element is 13.71. Here, the sf transition has the maximum contribution to the total strength and this is observed to be the norm in the case of other nuclei considered in Ref. [6] as well. Thus, from this single particle excitation method, the $GT^-$ centroid can be

TABLE IV. Experimental values of the energy centroids for $GT^+$ excitation in the mother nucleus and the values obtained from Eq. (5) and from the $M1$ method.

| Nucleus | $E_{GT^+}$ (MeV) (Expt.) | $E_{GT^+}$ (MeV) [Eq. (5)] | $M1$ config.[a] (daughter) | $E_{GT^+}$ (MeV) $(M1)$[b] |
|---|---|---|---|---|
| $^{54}$Fe | 2.8 | 3.05 | $(\pi^5_{f_{7/2}}),(\nu_{f_{5/2}},0_{p_{3/2}})$ | 5.17(4.07) |
| $^{56}$Fe | 2.3 | 2.62 | $(\pi^5_{f_{7/2}}),(\nu_{f_{5/2}},\nu^2_{p_{3/2}})$ | 4.44(4.60) |
| $^{59}$Co | 4.3 | 3.97 | $(\pi^6_{f_{7/2}}),(\nu_{f_{5/2}},\nu^4_{p_{3/2}})$ | 6.29(5.34) |

[a]The single particle shell model configurations [27] for the outermost levels of the daughter in the $M1$ excited state (Seeger neutron levels for both protons and neutrons).
[b]The numbers quoted within parentheses are the $E^+_{GT}$ values from the $M1$ method when the separate Seeger [27] levels are used for neutrons and protons.

expected to lie at 10.58 MeV. The experimental centroid lies at 10.75 MeV. However, as this method does not take into account the collective particle-hole excitations [8] of the nucleus (where a good fraction of the total strength can be expected to lie), it should not be expected to yield the experimental $E_{GT}$ precisely. This is a purely theoretical method, and the excitation energies are calculated from single particle shell model energy levels [27]. For the single particle levels of neutrons we have used the sequence and values labeled "Seeger" in Ref. [27]. Although for the protons the "Seeger" sequence lists $2p_{3/2}$ higher than $1f_{5/2}$, since the observed ground-state spins of $^{63}$Cu, $^{65}$Cu, etc. (where there is one extra proton beyond the $1f_{7/2}$ level) contradict this sequencing [i.e., the g.s. $J^\pi$ for these nuclei is $(3/2)^-$ and not $(5/2)^-$], following an earlier work [4] we adopt the same values for the proton single particle energy differences as in the case of neutrons in this work unless specifically mentioned otherwise.

Now, it is seen from the selection rules that most of the GT strength for nuclei with $A \simeq 60$ lies in the spin-flip transitions. Experimentally, too, it is observed that the sf transition strength is more concentrated than the nsf transition strength. For the sf transitions, the action of the GT operator is equivalent to a sf transition followed by an isospin flip ($M1$ transition from the mother to the daughter). If we consider a $T^<$ to $T^>$ transition, to find $E_{GT^+}$ in the daughter by the $M1$ method, we need to consider the $M1$ $\tau^-$ transition

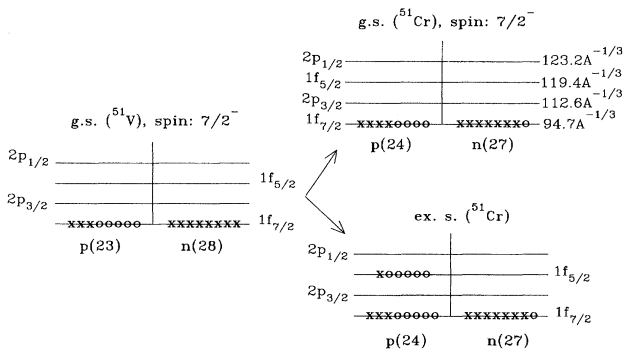


FIG. 6. Schematic diagram of single particle excitations illustrating the application of the FFN method to determination of $GT^-$ strength centroid with respect to the g.s. of $^{51}$Cr in $\beta^-$ decay of $^{51}$V. The level spacings are not drawn to scale.

from the daughter to the mother nucleus. The $M1$ method for finding the $GT^+$ centroid in the neutron-rich daughter nucleus (see, e.g., [6]) is based on the observation that most of the GT sf configuration strength is concentrated near the anti-isobaric analog state (AIAS) of the $M1$ giant resonance—the so-called $M1$-AIAS state. Now, the predominant configuration in the $M1$-AIAS state in the daughter is the spin-flip configuration generated from a $T^<$ mother ground state by transforming a proton in the $j=l+1/2$ state into an empty neutron in the $j=l-1/2$ level. The spin-flip configuration in the daughter is therefore the starting point and it is this configuration whose excitation with respect to the g.s. would yield the sought-for GT centroid. The $M1$ method generates, in the $T^<$ mother, the $T^>$ analog of this sf configuration by the application of the $T^+=\Sigma^A_{i=1}\tau^+_i$ (isospin-raising) operator. In general, there may be more than one AIAS of the sf configuration which are orthogonal to each other. These AIAS states contain most of the $M1$ excitation configuration strength and their energy can be calculated from the single particle shell model, taking into account the particle-hole repulsion energy and the pairing energy wherever relevant. The $T^>$ analog state is separated upwards from the AIAS states by the Lane potential. Once the energy of this $T^>$ analog state in the mother (of the sf configuration in the daughter) is known, subtraction of the energy of the analog state corresponding to the g.s. of the daughter ("the first analog") would yield the approximate excitation energy of the sf configuration in the $T^>$ daughter with respect to its g.s., which is the required $GT^+$ centroid in the daughter. This assumes an argument similar to the Brink hypothesis, as discussed later. The first analog state in the mother is often known experimentally, and where available this is an advantage in the $M1$ method.

As an illustration of this method, we consider the case of the $GT^+$ centroid in $^{54}$Mn [for the $^{54}$Fe$(e^-, \nu_e)$ $^{54}$Mn reaction]. Figure 7(a) shows the g.s. configuration of the mother nucleus $^{54}$Fe. The spin-flip excitation of $^{54}$Mn is shown in Fig. 7(b) and alongside it are shown the excited states of $^{54}$Fe which are obtained by operating $\tau^-$ on the spin-flip state of $^{54}$Mn. Thus the GT excitation corresponding to the sf excitation in Fig. 7(b) (in $^{54}$Mn) will be a superposition of the two basis configurations shown. Now, the AIAS corresponding to these two configurations can be constructed and its position in energy is determined as the weighted sum of the single particle excitation energies and the Lane potential (3.70 MeV for this case). The weighting factors obtained

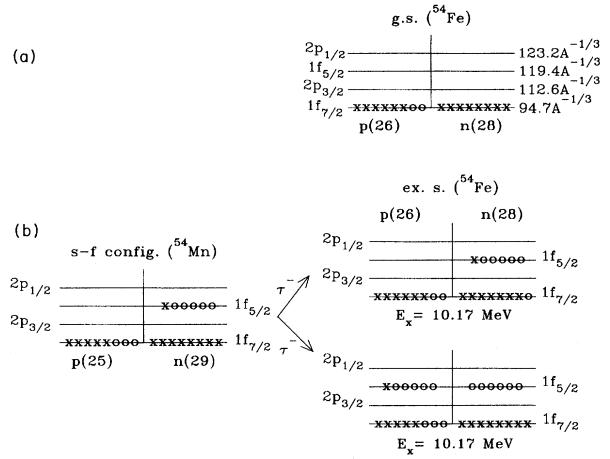


FIG. 7. The $M1$ method for $^{54}$Fe$(e^-, \nu_e)^{54}$Mn. (a) shows the g.s. configuration of $^{54}$Fe. In (b), the diagram on the left represents a spin-flip excitation in $^{54}$Mn generated from $^{54}$Fe g.s. by transforming a $1_{f_{7/2}}$ proton into a $1_{f_{5/2}}$ neutron. The IAS for the $^{54}$Fe configuration is a $\{\sqrt{3/4}, \sqrt{1/4}\}$ superposition of the shown basis states on the right; the AIAS state is similarly $\{-\sqrt{1/4}, \sqrt{3/4}\}$. The AIAS is separated from the IAS only by the Lane potential.

from the $M1$ method for the $^{54}$Fe excited state configurations are $\sqrt{3/4}$ and $\sqrt{1/4}$, respectively (see Fig. 7) and the excitation energies for each configuration in Fig. 7(b) are noted below them. The position of the GT excitation corresponding to the sf configuration of $^{54}$Mn will then be given by the difference in the energy of the obtained IAS state and the IAS state in $^{54}$Fe corresponding to the g.s. of $^{54}$Mn (the so-called first analog state—located at an excitation energy of 8.7 MeV—see below).

A few examples of the $M1$ method in $T^<$ to $T^>$ transitions are given in Table IV. For all the nuclei quoted in Table IV, the required $E_{\rm IAS}$ in the mother is known from experiment. For the mother nuclei quoted in Table III the $E_{\rm IAS}$ of the daughter ground states were obtained from [28] ($^{56}$Fe) and [29] ($^{59}$Co) and are 11.51 and 9.55 MeV, respectively. For $^{54}$Fe we note that Ref. [30] gives only the isobaric analog states corresponding to a few excited levels of $^{54}$Mn. The difference of the IAS energies and the corresponding levels in $^{54}$Mn is in the range of 8.59 to 8.79 MeV. Using the assumption (similar to the Brink hypothesis in electromagnetic transitions—see [5]) that the energies in the resonance states scale in the same way as those of the discrete states in the daughter, we adopt the mean value of 8.7 MeV as the $E_{\rm IAS}$ in $^{54}$Fe corresponding to the g.s. of $^{54}$Mn. The numbers quoted in the last column of Table IV are for IAS states giving GT energy closest to the experimentally observed GT centroid.

For the nuclei under consideration, the experimental inputs coupled with the given theoretical prescriptions ($M1$ and FFN methods) give numbers which can be compared with the empirical relations obtained here. Tables III and IV show that the empirically fitted values of $E_{\rm GT+}$ and $E_{\rm GT-}$ as reported in Sec. III are somewhat closer to the experimental centroids than the numbers obtained from the $M1$ and FFN methods. The results of Secs. II and III can therefore be used to calculate the weak transition properties of $f$-$p$shell nuclei of interest to astrophysics.

TABLE V. Coupling constants $\kappa_\tau$ and $\kappa_{\sigma\tau}$ for Bohr-Mottelson two particles interaction.

| Authors | Nuclei | $A\kappa_\tau$ | $A\kappa_{\sigma\tau}$ | $A(\kappa_\tau - \kappa_{\sigma\tau})$ |
|---|---|---|---|---|
| Gaarde [8] | $^{208}$Pb | 28 | 23 | 5 |
| Suzuki [33] | $^{90}$Zr | 32.5[a] | 25.9–28.6 | 3.92 |
| Suzuki [33] | $^{208}$Pb | 32.5[a] | 28.1–29.0[a] | 3.95 |
| Nakayama *et al.* [26] | "Global" fit $^{92}$Zr to $^{208}$Pb | 32.5 | 23.25 | 9.25 |
| This work | $f$-$p$ shell | 49.0 | 11.2 | 37.8 |

[a]Bohr-Mottelson estimate, quoted in [33].

## V. GT COLLECTIVE STATES FROM DISPERSION RELATIONS WITH BOHR-MOTTELSON HAMILTONIAN

Attempts have been made in the past to obtain a simple mass formula for the GT$^-$ energy systematics using the single particle level structure and two particle Bohr Mottelson type interaction Hamiltonians. The GTGR and the IAS states can be considered to be collective excitations excited by the spin-dependent and charge-exchange $\Sigma_{i=1}^A \tau_-^i \sigma^i$ and $\Sigma_{i=1}^A \tau_-^i$ operators. More specifically, in the GT$^-$ direction, the energy difference $E_{\rm GT} - E_{\rm IAS}$ can be written as (see, e.g., [31]):

$$E_{\rm GT^-} - E_{\rm IAS} = \frac{\langle \pi | \Sigma_{i=1}^A \tau_+^i \sigma_+^i H \Sigma_{j=1}^A \tau_-^j \sigma_-^j | \pi \rangle}{\langle \pi | \Sigma_{i=1}^A \tau_+^i \sigma_+^i \Sigma_{j=1}^A \tau_-^j \sigma_-^j | \pi \rangle} - \frac{\langle \pi | \Sigma_{i=1}^A \tau_+^i H \Sigma_{j=1}^A \tau_-^j | \pi \rangle}{\langle \pi | \Sigma_{i=1}^A \tau_+^i \Sigma_{j=1}^A \tau_-^j | \pi \rangle} .$$

The following form of the two particle interaction Hamiltonian [32] for example has been used here by various authors (e.g., Refs. [26], [31], and [33]):

TABLE VI. The distribution of $B_{\rm GT}^-$ strength of the spin-flip (sf) and no-spin-flip (nsf) transitions. Column 4 gives the fractional strength of the sf transitions.

| Nucleus | $B_{\rm GT}^-$ (nsf) | $B_{\rm GT}^-$ (sf) | $f$ |
|---|---|---|---|
| $^{51}$V | 6.42 | 13.71 | 0.68 |
| $^{81}$Br | 10.13 | 14.47 | 0.59 |
| $^{71}$Ga | 6.60 | 15.04 | 0.69 |
| $^{54}$Fe | 2.57 | 13.71 | 0.84 |
| $^{58}$Ni | 3.33 | 16.37 | 0.83 |
| $^{56}$Fe | 5.90 | 16.37 | 0.73 |
| $^{60}$Ni | 0.0 | 19.04 | 1.00 |

$$H=-\sum_{i=1}^{A}\xi_i l_i\sigma_i+\frac{1}{2}\kappa_\tau\sum_{i\neq j}\tau_i\cdot\tau_j+\frac{1}{2}\kappa_\sigma\sum_{i\neq j}\sigma_i\cdot\sigma_j+\frac{1}{2}\kappa_{\sigma\tau}\sum_{i\neq j}(\tau_i\cdot\tau_j)(\sigma_i\cdot\sigma_j)$$

where $\kappa_\sigma$, $\kappa_\tau$, and $\kappa_{\sigma\tau}$ are the coupling constants (divided by the mass number) for the spin-spin, isospin-isospin, and the spin-isospin interaction terms and $\xi_i$ is the single particle spin-orbit coupling constant. Using the simplification brought about by considering the case of very neutron-rich nuclei where the Tamm-Dancoff approximation would be valid and further considering only nuclei for which the protons occupy the major shells and the neutrons fill the $j=l+1/2$ subshell, e.g., in the cases of $^{90}$Zr and $^{48}$Ca, Suzuki [33] has used the experimentally known values of $E_{\mathrm{GT}^-}-E_{\mathrm{IAS}}$ to determine the difference in the coupling constants $(\kappa_\tau-\kappa_{\sigma\tau})$ (see Table V).

Another approach (due to Gaarde [8]) to the GTGR energy systematics is from the field description of the coherent particle-hole excitations which lead to the GT resonance. In the field description, the coherent state is generated by an oscillation of the average field in the spin-isospin state which is propotional to $\sigma\tau$. The self-consistency condition on this oscillating potential leads to a dispersion relation for the energy of the GT collective state. Further, if it is assumed that the strength is clustered mainly around two regions, one corresponding to the no-spin-flip transitions with energy $\epsilon_i$ and the other to the spin-flip transitions with energy $\epsilon_i+\Delta_{ls}$, then the energy dispersion relation equivalent to a random-phase approximation (RPA) equation for a separable force can be written as

$$\frac{2(N-Z)(1-f)}{\epsilon_i-\epsilon}+\frac{2(N-Z)f}{\epsilon_i+\Delta_{ls}-\epsilon}=\frac{-1}{\kappa_{\sigma\tau}} \tag{6}$$

where $f$ is the fraction of the total strength lying in the spin-flip region, and $\Delta_{ls}$ is the spin-orbit splitting energy. The quantity $f$ is evaluated for each of the nuclei [for which $(p,n)$ data exist] from the single particle transition configurations constructed using the FFN method and is tabulated in Table VI. A similar expression may be developed for the IAS transition which has the form

$$\epsilon_{\mathrm{IAS}}-\epsilon_{i,\mathrm{IAS}}=2\kappa_\tau(N-Z). \tag{7}$$

Using the experimentally known values of $E_{\mathrm{IAS}}$ and Eq. (7), we obtain the value of $\kappa_\tau$ as $49.04/A$ and $\epsilon_{i,\mathrm{IAS}}=-3.48$. Keeping this value of $\kappa_\tau$ fixed, the "experimental" values of $E^-_{\mathrm{GT}}$ and $E_{\mathrm{IAS}}$ obtained from Table III and Fig. 3 are fitted by a two parameter least square fit to the quantity $(\epsilon_{\mathrm{GT}}-\epsilon_{i,\mathrm{GT}})-(\epsilon_{\mathrm{IAS}}-\epsilon_{i,\mathrm{IAS}})$, where the first term is evaluated from the quadratic roots of Eq. (6). This gives the value of $\kappa_{\sigma\tau}$ as $11.16/A$ and $\epsilon_{i,\mathrm{GT}}=6.49$. As is shown in Table V, these values differ from those obtained for $^{208}$Pb, or even for the $^{90}$Zr region, indicating that in order to explain both the IAS and GT energetics the simple Bohr-Mottelson Hamiltonian requires coupling coefficients which are substantially different for different shells. At the same time it is not surprising that the relation (4) developed for $f$-$p$ shell nuclei which can be shown to depend on the coupling constants (as in the approach of Suzuki [31,33]) would differ substantially from similar relations [26] developed for a different region of the isotope table.

## VI. CONCLUSION

Since the spectral distribution theory is essentially a statistical theory requiring the existence of a large number of basis states, this approach is expected to be valid only for nuclei which are far removed from the closed shell and subshell configurations. Using the framework of the spectral distribution theory, we have used the experimental data on charge-exchange reactions on $fp$ shell nuclei to obtain the energy centroid of the collective Gamow-Teller resonances for arbitrary nuclei in this shell. These quantities, together with the prediction of total GT strength (such as given in [23]) are useful in the prediction of reaction rates mediated by weak interactions in the cores of massive presupernova stars. We have in Eqs. (4) and (5) a dependence of the GT energy centroids in the $f$-$p$ shell on the spin-orbit interaction, the Lane potential, and the pairing energy. Further, with a view to comparing the implications of the experimental results for $fp$ shell nuclei with earlier work on heavier nuclei (see [8], [26], and [31]) we have used the experimental values of the GT$^-$ centroids and the IAS energies to extract the relevant coupling coefficients in the Bohr-Mottelson Hamiltonian, for the $f$-$p$ shell. The fact that they differ from those of the earlier studies for heavier nuclei such as in the region of $^{208}$Pb indicates that apart from the $1/A$ dependence there may be an intrinsic shell dependence of these coupling constants when a simple model like the one due to Bohr-Mottelson has to be used.

The results of these calculations are being used to predict the neutrino energy spectrum during the collapse phase up to the point of $\nu_e$ trapping. In the event of a sufficiently nearby supernova explosion, these can be compared with the neutrino spectroscopy results obtainable by future neutrino detectors (e.g., SNO, ICARUS) — thereby revealing clues to the important thermodynamic and nuclear conditions of the presupernova core. A preliminary discussion of this was reported in Ref. [34].

*Note added.* After this work was accepted for publication, a paper on experimental GT$_+$ strength distributions in $^{60}$Ni, $^{62}$Ni, and $^{64}$Ni by Williams *et al.* [Phys. Rev. C **51**, 1144 (1995)] came to our notice. Using their experimental data, we find that the strength-weighted energy centroids for these nuclei are at 2.59, 2.56, and 2.8 MeV, respectively. This is to be compared with our predictions [from Eq. (5)] of 2.59, 2.21, and 1.86 MeV. While the predictions of Eq. (5) [based on the $(n,p)$ data of the earlier seven nuclei] are reasonably good for $^{60}$Ni and $^{62}$Ni, it does not work well in the case of $^{64}$Ni, possibly because in the latter nucleus much of the strength is concentrated in the ground state to ground state transition.

## ACKNOWLEDGMENTS

We thank K. Kar and S. Sarkar for the initial impetus to work on this problem. This research formed a part of the 8th Five Year Plan (8P-45) at Tata Institute.

[1] G. E. Brown, H. A. Bethe, and G. Baym, Nucl. Phys. **A375**, 481 (1982).
[2] H. A. Bethe, G. E. Brown, J. Applegate, and J. M. Lattimer, Nucl. Phys. **A324**, 487 (1979).
[3] G. Fuller, Astrophys. J. **252**, 741 (1982).
[4] K. Kar, A. Ray, and S. Sarkar, Astrophys. J. **434**, 662 (1994).
[5] H. V. Klapdor, in Proceedings of the Third International Conference on Nuclei Far from Stability, CERN-Report No. 76-13, 1976.
[6] G. M. Fuller, W. A. Fowler, and M. J. Newman, Astrophys. J. **252**, 715 (1982).
[7] D. J. Horen *et al.*, Phys. Lett. **99B**, 383 (1981).
[8] C. Gaarde, Nucl. Phys. **A396**, 127 (1983).
[9] T. N. Taddeucci *et al.*, Nucl. Phys. **A469**, 125 (1987).
[10] J. Rapaport *et al.*, Nucl. Phys. **A410**, 371 (1983).
[11] M. C. Vetterli *et al.*, Phys. Rev. C **40**, 559 (1989).
[12] D. Krofcheck *et al.*, Phys. Lett. B **189**, 299 (1987).
[13] J. Rapaport *et al.*, Nucl. Phys. **A427**, 332 (1984).
[14] D. Krofcheck *et al.*, Phys. Rev. Lett. **55**, 1051 (1985).
[15] W. P. Alford, A. Celler, B. A. Brown, R. Abegg, K. Ferguson, R. Helmer, K. P. Jackson, S. Long, K. Raywood, and S. Yen, Nucl. Phys. **A531**, 97 (1991).
[16] S. El-Kateb *et al.*, Phys. Rev. C **49**, 3128 (1994).
[17] W. P. Alford *et al.*, Phys. Rev. C **48**, 2818 (1993).
[18] M. C. Vetterli *et al.*, Phys. Rev. C **45**, 997 (1992).
[19] K. J. Raywood *et al.*, Phys. Rev. C **41**, 2836 (1990).
[20] W. P. Alford *et al.*, Nucl. Phys. **A514**, 49 (1990).
[21] T. N. Taddeucci *et al.*, Phys. Rev. C **25**, 1094 (1981).
[22] M. B. Aufderheide, S. Bloom, D. A. Resler, and G. J. Mathews, Phys. Rev. C **47**, 2961 (1993).
[23] S. E. Koonin and K. Langanke, Phys. Lett. B **326**, 5 (1994).
[24] J. B. French and V. K. B. Kota, Annu. Rev. Nucl. Part. Sci. **32**, 35 (1982).
[25] V. K. B. Kota and K. Kar, Pramana **32**, 647 (1989).
[26] K. Nakayama, A. Pio Galleão, and F. Krmpotić, Phys. Lett. **114B**, 217 (1982).
[27] M. Hillman and J. R. Grover, Phys. Rev. **185**, 1307 (1969).
[28] H. Junde, H. Dailing, Z. Chunmei, H. Xiaoling, H. Baohua, and W. Yaodong, Nucl. Data Sheets **51**, 1 (1987).
[29] P. Andersson, L. P. Ekström, and J. Lyttkens, Nucl. Data Sheets **69**, 733 (1993).
[30] W. Gongqing, Z. Jaibi, and Z. Jingen, Nucl. Data Sheets **50**, 255 (1987).
[31] T. Suzuki, Nucl. Phys. **A379**, 110 (1982).
[32] A. Bohr and B. R. Mottelson, Phys. Lett. **100B**, 10 (1981).
[33] T. Suzuki, Phys. Lett. **104B**, 92 (1981).
[34] F. K. Sutaria and A. Ray, in *Proceedings of "Nuclei in Cosmos," 3rd International symposium on Nuclear Astrophysics*, edited by M. Busso, R. Gallino, and C. Raiteri, AIP Conf. Proc. No. 327 (AIP, New York, 1994), p. 187.